Large-scale Modeling of The Non-linear Enzymatic Reaction Kinetics to Optimize Engineered Pentose Fermentation in *Zymomonas mobilis*

M. Mete Altintas[1], Christina Eddy[2], Min Zhang[2], James D. McMillan[2] and Dhinakar S. Kompala[1]

1. Chemical and Biological Engineering Dept, University of Colorado, Boulder
2. Biotechnology Division for Fuels and Chemicals, NREL, Golden, CO

Background

Zymomonas mobilis has been engineered with 4 new enzymes to ferment xylose along with glucose and a network of pentose pathway enzymatic reactions interacting with the native glycolytic Entner Doudoroff pathway has been hypothesized.

We investigated this proposed reaction network by developing a kinetic model for all the enzymatic reactions of the pentose phosphate and glycolytic pathways.

Kinetic data on different sugar metabolism rates and enzymatic activity data was used to refine the model parameters available in the literature and validate the proposed reaction network.

Objectives

- To investigate the assumed network of enzymatic reactions linking the pentose metabolism and glycolysis pathways.
- To incorporate the non-linear rate expressions for the feedback regulation of enzymatic reactions.
- To find an optimum combination of enzymes needed for maximizing ethanol concentration.

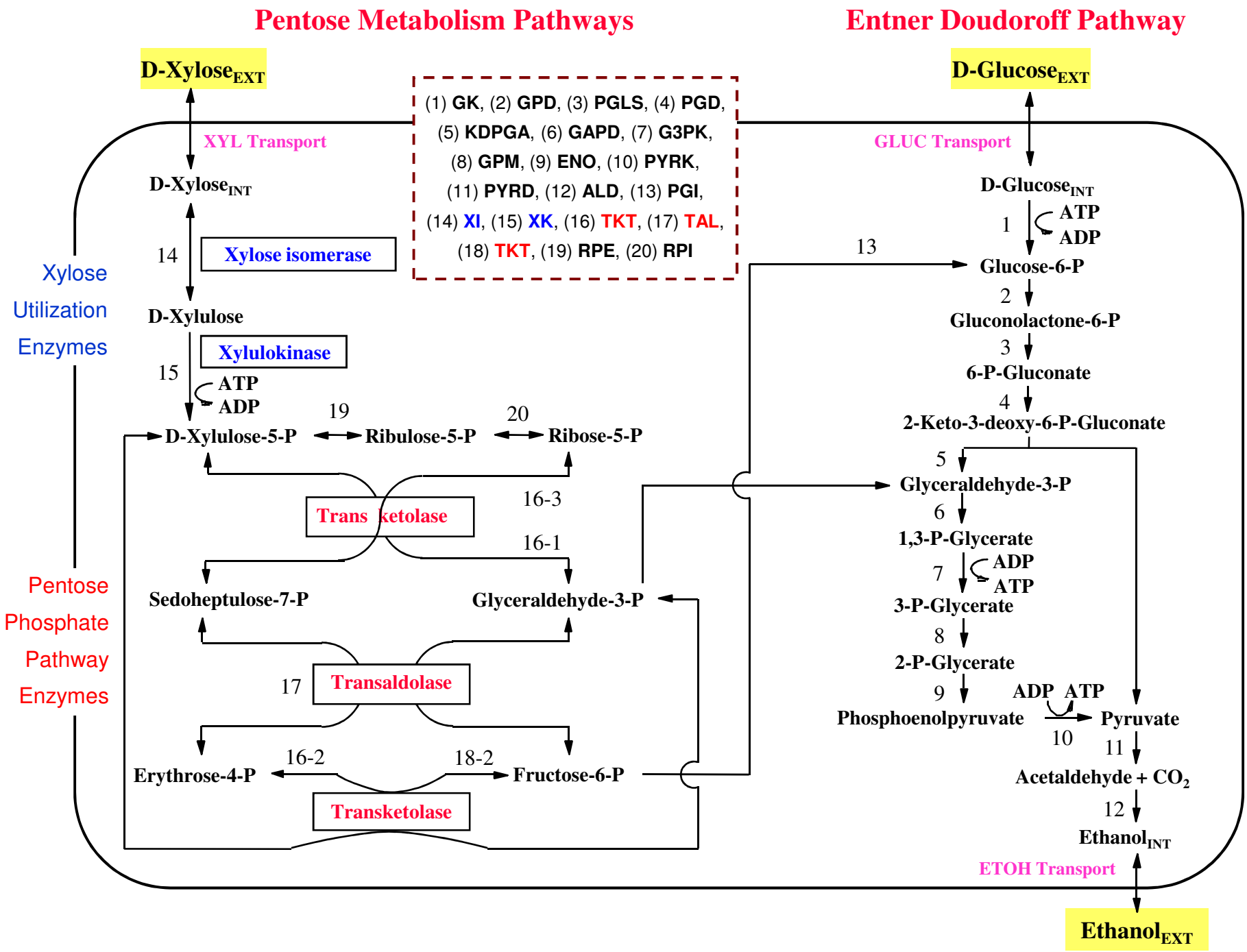
Pentose Metabolism Pathways
Entner Doudoroff Pathway
D-Xylose$_{EXT}$
D-Glucose$_{EXT}$
(1) GK, (2) GPD, (3) PGLS, (4) PGD,
(5) KDPGA, (6) GAPD, (7) G3PK,
(8) GPM, (9) ENO, (10) PYRK,
(11) PYRD, (12) ALD, (13) PGI,
(14) XI, (15) XK, (16) TKT, (17) TAL,
(18) TKT, (19) RPE, (20) RPI
XYL Transport
GLUC Transport
D-Xylose$_{INT}$
D-Glucose$_{INT}$
Xylose Utilization Enzymes
14
Xylose isomerase
D-Xylulose
15
Xylulokinase
ATP
ADP
19
20
D-Xylulose-5-P
Ribulose-5-P
Ribose-5-P
16-3
Trans ketolase
16-1
Sedoheptulose-7-P
Glyceraldehyde-3-P
Pentose Phosphate Pathway Enzymes
17
Transaldolase
16-2
18-2
Erythrose-4-P
Fructose-6-P
Transketolase
1
ATP
ADP
13
Glucose-6-P
2
Gluconolactone-6-P
3
6-P-Gluconate
4
2-Keto-3-deoxy-6-P-Gluconate
5
Glyceraldehyde-3-P
6
1,3-P-Glycerate
7
ADP
ATP
3-P-Glycerate
8
2-P-Glycerate
9
ADP ATP
Phosphoenolpyruvate
10
Pyruvate
11
Acetaldehyde + CO_2
12
Ethanol$_{INT}$
ETOH Transport
Ethanol$_{EXT}$

Features of Kinetic Modeling

- The mechanistic rate equations for each of the enzymatic reactions occurring inside the cell mass.

- The rate equations for the transport of major substrates into cells and of major products out of the cells.

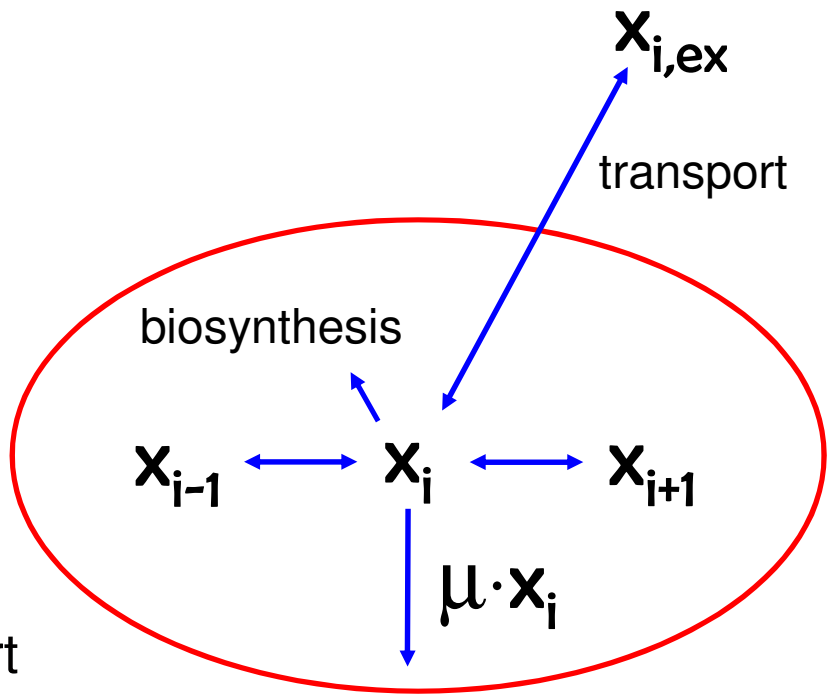

The *Zymomonas* System

#	ENZYME	REACTANTS	PRODUCTS	INHIBITORS	MECHANISM
1 (→)	Glucokinase	GLUC + ATP	GLUC6P + ADP	GLUC6P	Michaelis-Menten
2 (→)	Glucose-6-P dehydrogenase	GLUC6P + NAD(P)	PGL + NAD(P)H	ATP	Michaelis-Menten
3 (→)	6-phosphogluconolactonase	PGL	PG	GLUC6P	Michaelis-Menten
4 (→)	6-phosphogluconate dehydratase	PG	KDPG	G3P	Michaelis-Menten
5 (→)	2-keto-3-deoxy-6-P-gluconate aldolase	KDPG	GAP + PYR		Michaelis-Menten
6 (↔)	Glyceraldehyde-3-P dehydrogenase	GAP + NAD	DPG + NADH		M.-Menten & Rev.
7 (↔)	3-phosphoglycerate kinase	DPG + ADP	G3P + ATP		M.-Menten & Rev.
8 (→)	Phosphoglycerate mutase	G3P	G2P		Michaelis-Menten
9 (→)	Enolase	G2P	PEP		Michaelis-Menten
10 (→)	Pyruvate kinase	PEP + ADP	PYR + ATP		Michaelis-Menten
11 (→)	Pyruvate decarboxylase	PYR	ACET		Michaelis-Menten
12 (↔)	Alcohol dehydrogenase	ACET + NADH	ETOH + NAD		M.-Menten & Rev.
13 (→)	Phosphoglucose isomerase	FRUC6P	GLUC6P	PG	Michaelis-Menten
14 (→)	Xylose isomerase	XYL	XYLU		Michaelis-Menten
15 (→)	Xylulokinase	XYLU + ATP	XYLU5P + ADP		Michaelis-Menten
16 (↔)	Transketolase	XYLU5P + RIB5P	SED7P + GAP		M.-Menten & Rev.
17 (↔)	Transaldolase	SED7P + GAP	FRUC6P + E4P		Ping-Pong Bi Bi
18 (↔)	Transketolase	XYLU5P + E4P	FRUC6P + GAP		M.-Menten & Rev.
19 (↔)	Ribulose 5-phosphate epimerase	XYLU5P	RIBU5P		M.-Menten & Rev.
20 (↔)	Ribose 5-phosphate isomerase	RIBU5P	RIB5P		M.-Menten & Rev.

Approach

- The kinetic model developed to describe the *Zymomonas* system is comprised of 24 rate expressions and 24 balance equations.
- All the derivatives of balance equations were set to zero to calculate a steady state. The resulting system of non-linear equations was solved numerically for the steady state metabolite concentrations.
- The amounts of 5 enzymes (PGI, XI, XK, TKT and TAL) were varied such that the total of ED and PP pathway enzymes ranges from 42% to 66% of the total cellular protein.
- The k_{cat} values reported at varying temperatures are normalized by using the 'glucose consumption vs. temperature' table presented by Scopes and Griffiths-Smith (1986) to estimate the k_{cat} values at 30°C.

Assumptions and Conditions

- The k_{cat} and K_m values used in the model were collected from the literature at varying pH's.
- The concentrations of ATP, ADP, NAD, NADH and NADP were assumed to be constant and equal to 2, 1, 1.5, 1 and 0.5 mM, respectively.
- A constant level of gene expression was assumed, i.e. the enzyme levels that were measured in the wild-type strain were used.
- For the heterologous enzymes, k_{cat} and K_m values from *E. coli* were used.

- Xylose and glucose are constant at 5.0 and 0.875 g/L, respectively.
- The chemostat is operated at a constant dilution rate of 0.05 h^{-1}.
- The cell mass concentration in the bioreactor is constant at 1.0 g/L.
- The cytoplasmic volume of *Zymomonas* cells growing in the presence of glucose and xylose were taken to be 2.2 ml/g dcm.

Sample Rate Expression

$$\upsilon_1 = \frac{k_{cat} \cdot [E]_T \times \left(\frac{GLUC}{K_{m,GLUC}}\right) \times \left[\frac{ATP}{K_{m,ATP} \times \left(1 + \frac{GLUC6P}{K_{i,GLUC6P}}\right)}\right]}{1 + \frac{GLUC}{K_{m,GLUC}} + \frac{ATP}{K_{m,ATP}} + \frac{GLUC \times ATP}{K_{m,GLUC} \times K_{m,ATP} \times \left(1 + \frac{GLUC6P}{K_{i,GLUC6P}}\right)} + \frac{GLUC6P}{K_{i,GLUC6P}}}$$

2 Sub.s + 2 Prod.s

Michaelis-Menten Mech.

Irreversible Rxn.

Competitive product inhibiton term

- K_{cat}, K_m and K_i values are reported in the literature
- $\upsilon_{max} = k_{cat} \cdot [E]_T$
- $[E_T]$ = (g enzyme/g total protein) x (g protein/g dry cell)

Representative Balance Equations

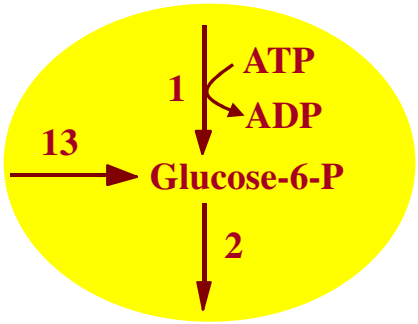

$$\frac{d[GLUC6P]}{dt} = (v_1 + v_{13} - v_2) - \mu \cdot [GLUC6P]$$

rate expressions

dilution due to growth

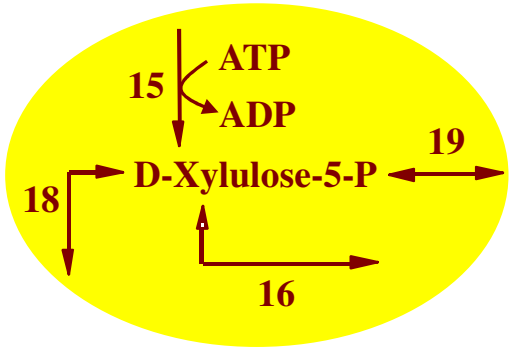

$$\frac{d[XYLU5P]}{dt} = (v_{15} - v_{16} - v_{18} - v_{19}) - \mu \cdot [XYLU5P]$$

METABOLITES

Metabolites	Dynamic Balance Equations (d[metabolite]/dt = …)	Steady State Intracellular Concentrations (mmol/g dry weight)
GLUC	$(\upsilon_{GLUC} - \upsilon_1) - (\mu \cdot GLUC)$	4.48×10^{-3}
GLUC6P	$(\upsilon_1 + \upsilon_{13} - \upsilon_2) - (\mu \cdot GLUC6P)$	4.70×10^{-3}
PGL	$(\upsilon_2 - \upsilon_3) - (\mu \cdot PGL)$	4.15×10^{-4}
PG	$(\upsilon_3 - \upsilon_4) - (\mu \cdot PG)$	7.97×10^{-4}
KDPG	$(\upsilon_4 - \upsilon_5) - (\mu \cdot KDPG)$	2.61×10^{-3}
GAP	$(\upsilon_5 + \upsilon_{16,1} - \upsilon_6 - \upsilon_{17} - \upsilon_{18,1}) - (\mu \cdot GAP)$	0.26
BPG	$(\upsilon_6 - \upsilon_7) - (\mu \cdot BPG)$	0.11
G3P	$(\upsilon_7 - \upsilon_8) - (\mu \cdot G3P)$	2.15×10^{-3}
G2P	$(\upsilon_8 - \upsilon_9) - (\mu \cdot G2P)$	4.68×10^{-3}
PEP	$(\upsilon_9 - \upsilon_{10}) - (\mu \cdot PEP)$	4.95×10^{-4}
PYR	$(\upsilon_5 + \upsilon_{10} - \upsilon_{11}) - (\mu \cdot PYR)$	1.28×10^{-2}
ACET	$(\upsilon_{11} - \upsilon_{12}) - (\mu \cdot ACET)$	0.14
ETOH	$(\upsilon_{12} - \upsilon_{ETOH}) - (\mu \cdot ETOH)$	192.10
XYL	$(\upsilon_{XYL} - v_{14}) - (\mu \cdot XYL)$	64.92
XYLU	$(\upsilon_{14} - \upsilon_{15}) - (\mu \cdot XYLU)$	7.92
XYLU5P	$(\upsilon_{15} + \upsilon_{18,1} - \upsilon_{16,1} - \upsilon_{19}) - (\mu \cdot XYLU5P)$	0.25
RIBU5P	$(\upsilon_{19} - \upsilon_{20}) - (\mu \cdot RIBU5P)$	0.27
RIB5P	$(\upsilon_{16,3} + \upsilon_{20} - \upsilon_{18,3}) - (\mu \cdot RIB5P)$	0.52
SED7P	$(\upsilon_{18,3} - \upsilon_{16,3} - \upsilon_{17}) - (\mu \cdot SED7P)$	7.94
E4P	$(\upsilon_{16,2} + \upsilon_{17} - \upsilon_{18,2}) - (\mu \cdot E4P)$	1.25×10^{-2}
FRUC6P	$(\upsilon_{17} + \upsilon_{18,2} - \upsilon_{13} - \upsilon_{16,2}) - (\mu \cdot FRUC6P)$	6.67×10^{-2}

Concentration Trajectories

PGI = 0.1%
XI = 4.6%
XK = 0.3%
TAL = 3.0%
TKTs = 0.4%

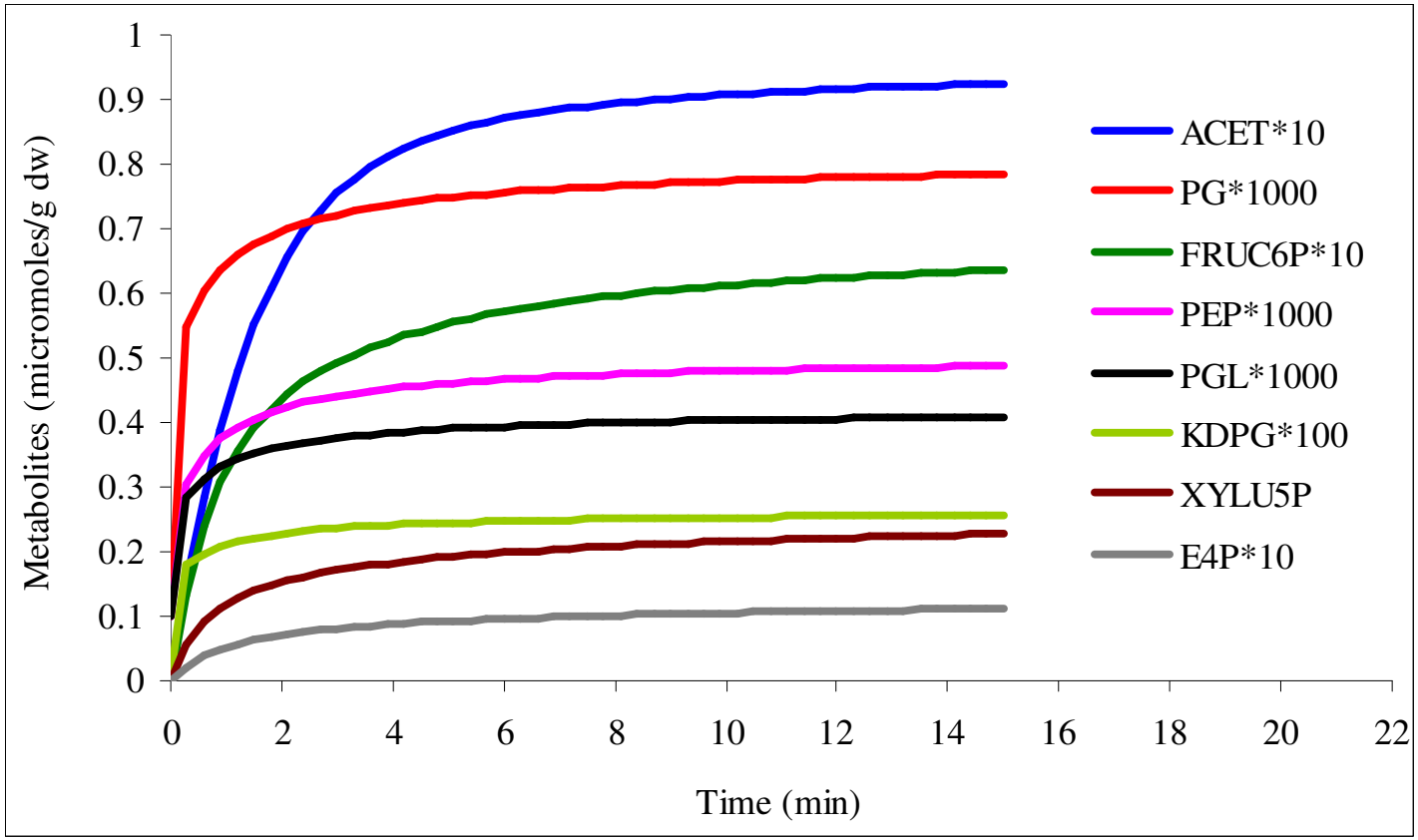

ACET: acetaldehyde
PG: 6-phosphogluconate
FRUC6P: fructose-6-phosphate
PEP: phosphoenolpyruvate
PGL: 6-phosphogluconolactone
KDPG: 2-keto-3-deoxy-6-phosphogluconate
XYLU5P: xylulose-5-phosphate
E4P: erythrose-4-phosphate

Maximum Ethanol Concentration & Optimal Ethanol Production Efficiency

PGI (%)	XI (%)	XK (%)	TAL (%)	TKTs (%)		Total Key Enzyme Expression Level (%)	ETOH (g/L)	ETOH / Key Enzyme Expression Level
				TKT	TKT-C_2			
Objective: Maximize ethanol concentration								
1.1	**9.0**	**3.7**	**6.1**	**0.8**	**4.1**	24.8	**6.1258**	0.2470
1.3	9.0	3.7	6.1	0.9	4.2	25.2	**6.1258**	0.2431
1.1	9.0	3.7	6.0	0.9	4.3	25.0	**6.1258**	0.2450
1.4	9.0	4.1	5.7	0.8	3.7	24.7	**6.1258**	0.2480
1.3	9.0	3.9	5.9	0.8	3.9	24.8	**6.1258**	0.2470
Objective: Optimize ethanol production efficiency								
0.1	**4.6**	**0.3**	**3.0**	**0.1**	**0.3**	8.4	6.1202	**0.7286**
0.1	4.6	0.3	3.1	0.1	0.2	8.4	6.1202	**0.7286**
0.1	4.6	0.3	2.9	0.2	0.3	8.4	6.1191	**0.7285**
0.1	4.6	0.3	3.1	0.1	0.3	8.5	6.1207	**0.7201**
0.1	4.6	0.3	3.2	0.1	0.2	8.5	6.1207	**0.7201**

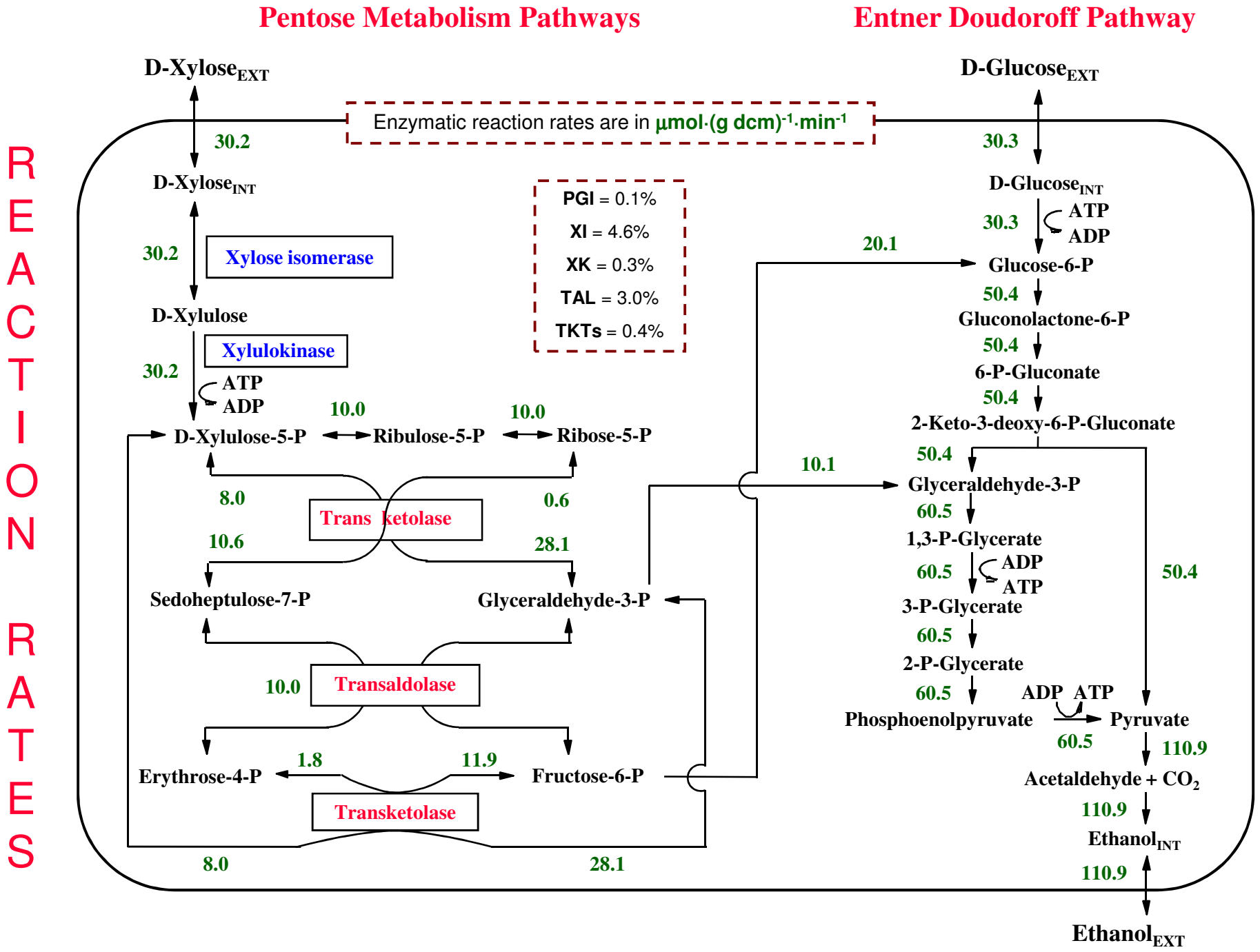
Pentose Metabolism Pathways
Entner Doudoroff Pathway
REACTION RATES
Enzymatic reaction rates are in µmol·(g dcm)-1·min-1
D-Xylose EXT
D-Xylose INT
D-Xylulose
D-Xylulose-5-P
Ribulose-5-P
Ribose-5-P
Sedoheptulose-7-P
Glyceraldehyde-3-P
Erythrose-4-P
Fructose-6-P
Xylose isomerase
Xylulokinase
Trans ketolase
Transaldolase
Transketolase
ATP
ADP
30.2
10.0
10.0
8.0
0.6
10.6
28.1
10.0
1.8
11.9
8.0
28.1
PGI = 0.1%
XI = 4.6%
XK = 0.3%
TAL = 3.0%
TKTs = 0.4%
D-Glucose EXT
D-Glucose INT
Glucose-6-P
Gluconolactone-6-P
6-P-Gluconate
2-Keto-3-deoxy-6-P-Gluconate
Glyceraldehyde-3-P
1,3-P-Glycerate
3-P-Glycerate
2-P-Glycerate
Phosphoenolpyruvate
Pyruvate
Acetaldehyde + CO2
Ethanol INT
Ethanol EXT
30.3
20.1
50.4
50.4
50.4
10.1
50.4
60.5
60.5
60.5
60.5
60.5
110.9
110.9
110.9

Impact of PGI, XI and XK Concentrations

PGI=0%, TAL=0.1%, TKTs=0.1%

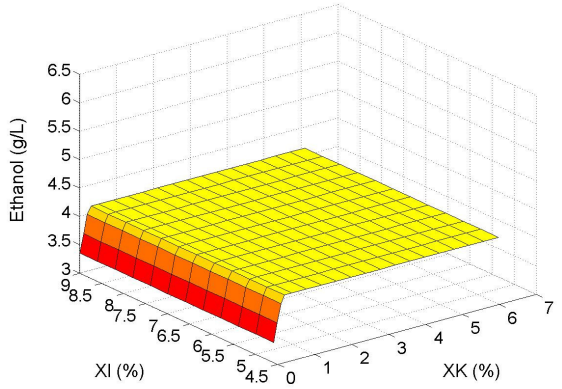

PGI=0%, TAL=6.1%, TKTs=0.1%

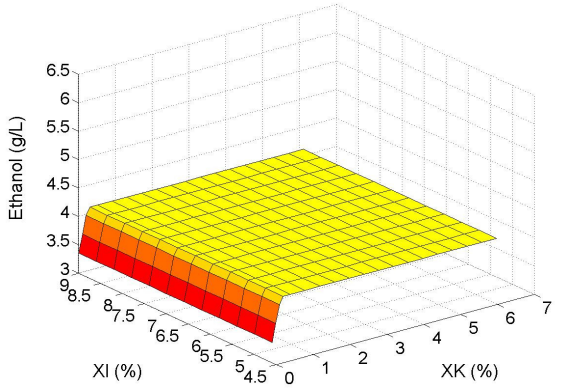

PGI=0%, TAL=6.1%, TKTs=6.1%

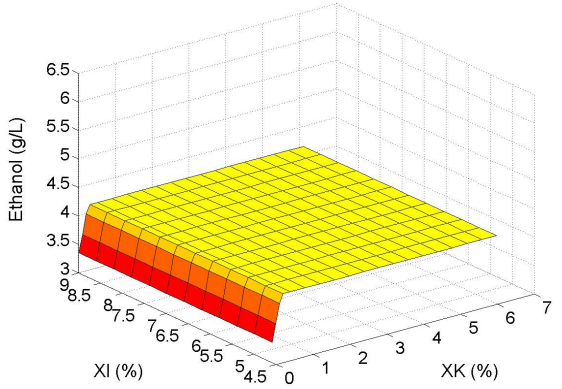

PGI=0.1-1.5%, TAL=0.1%, TKTs=0.1%

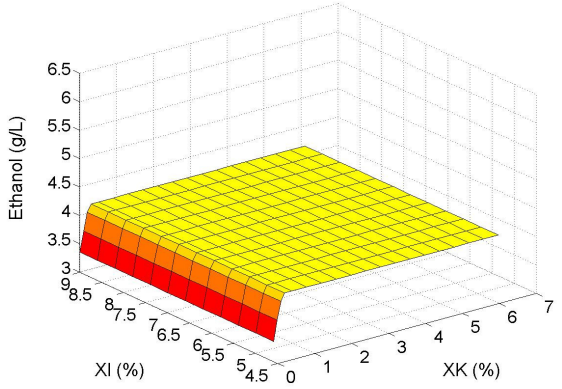

PGI=0.1-1.5%, TAL=6.1%, TKTs=0.1%

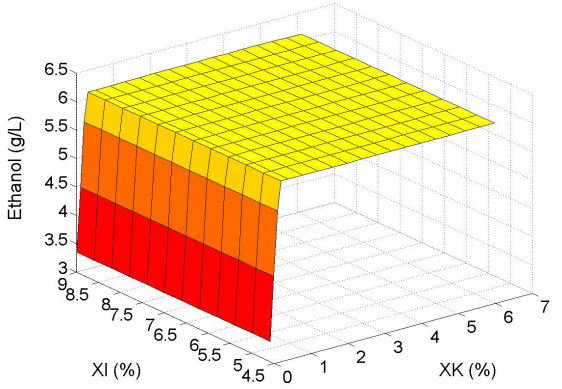

PGI=0.1-1.5%, TAL=6.1%, TKTs=6.1%

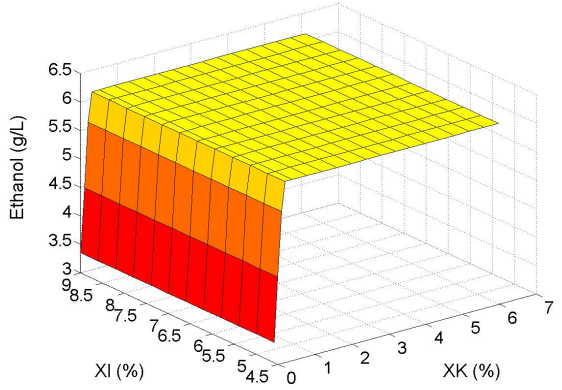

Impact of XI and XK Concentrations

Optimal concentrations of the key enzymes :

PGI = 0.1%

XI = 4.6%

XK = 0.3%

TAL = 3.0%

TKTs = 0.4%

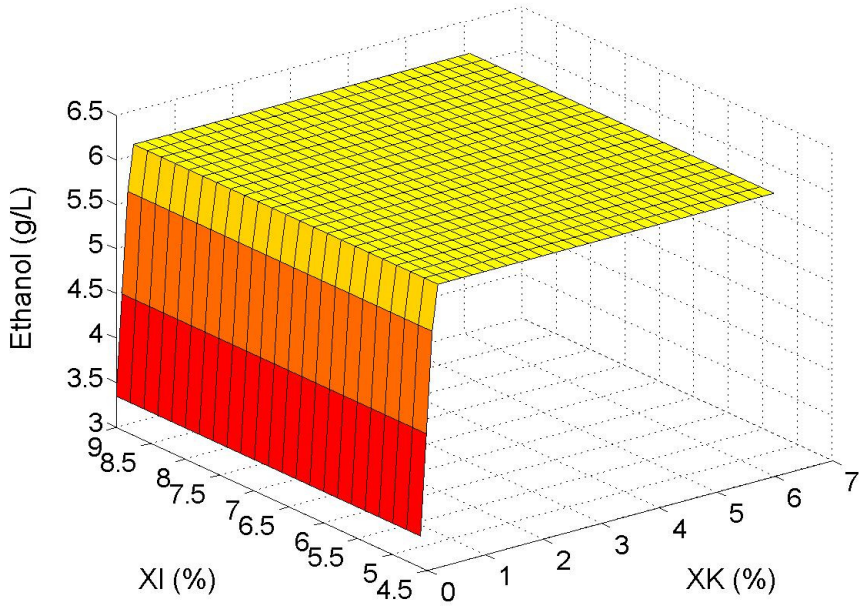

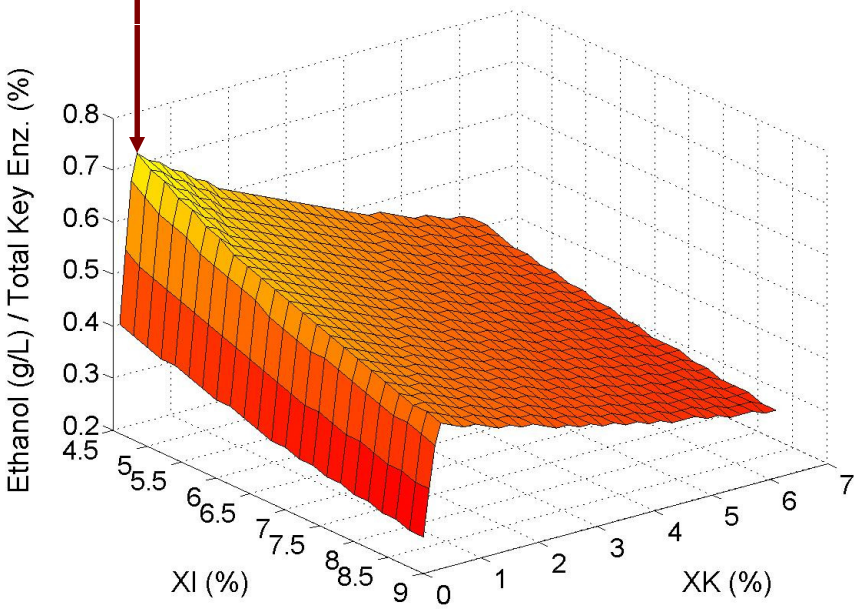

Impact of TAL and TKT Concentrations

PGI = 0.1%

XI = 4.6%

XK = 0.3%

TAL = 0.1%

TKTs = 0.1%

$ETOH_{EXT}$ = 4.15 g/L (only 68% of the maximum)

Optimal concentrations of the key enzymes :

PGI = 0.1%

XI = 4.6%

XK = 0.3%

TAL = 3.0%

TKTs = 0.4%

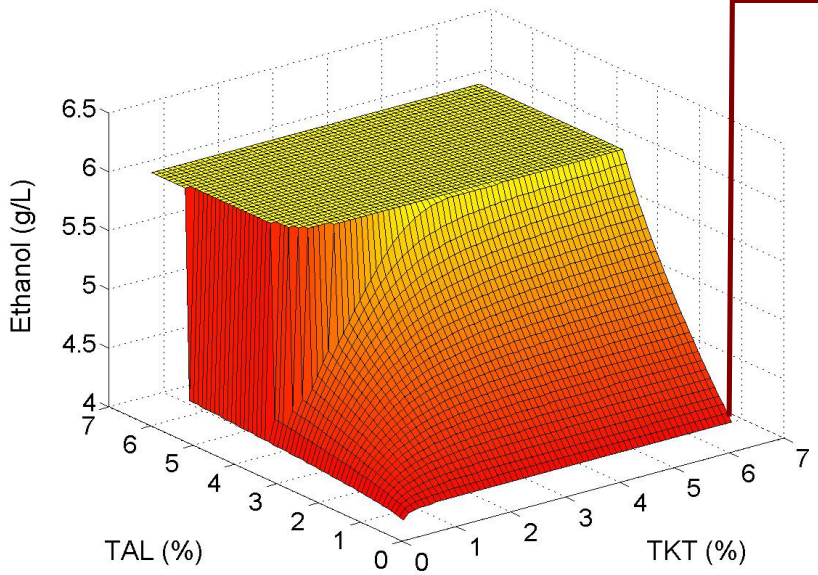

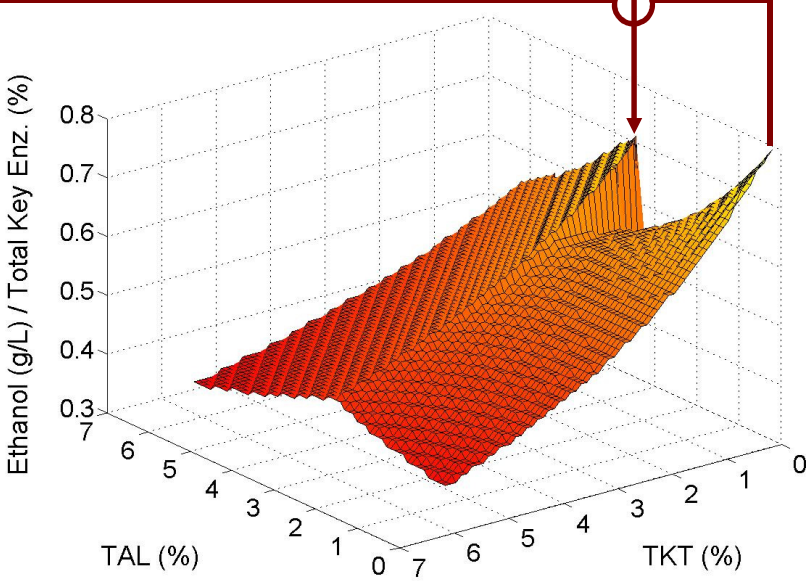

Results

- The kinetic model simulations at each enzyme combination produce enormous amount of information, including the steady state metabolite concentrations as well as the dynamic variations in the individual reaction rates for each enzymatic reaction and metabolite.
- Amongst the 5 enzymes whose amounts were tested in terms of the ethanol production, it was found that TAL, XI and XK were the most important enzymes in terms of their effect on the extracellular ethanol concentration. Their presence at sufficient levels eliminates pathway bottlenecks and significant accumulation of intermediate metabolites.
- The relatively low amounts of native PGI and heterologous TKT are sufficient to enable maximal ethanol production.

Results

- Since the reaction rates in the glycolysis pathway are higher than the rates in PP pathway, ‘glyceraldehyde 3-P’ is channeled quickly into the glycolysis pathway.
- Following the flow of ‘glyceraldehyde 3-P’ into the glycolysis pathway, the amounts of ‘erythrose 4-P’ and ‘fructose 6-P’ drops dramatically when TAL and TKT enzymes are available.
- The relatively slow rate of reactions in the PP pathway makes XI and XK enzymes important in terms of their ability to control the reactions immediately following xylose transport into the cell.

Conclusion

- The kinetic modeling strategy allows us to incorporate known information about non-linear rate equations and regulation by other metabolites in determining the optimum combination of heterologous enzymes to maximize pathway efficiency.
- The model enables us to compare the enzymatic reaction rates between the pentose utilization (PP) and glycolytic (ED) pathways and calculate the metabolic flux for each enzymatic reaction at all the assumed levels of heterologous enzymes.

Acknowledgements

This work was supported by the Office of the Biomass Program of the U.S. Department of Energy (DOE) and U.S. Department of Agriculture (USDA).

Large-scale Modeling of The Non-linear Enzymatic Reaction Kinetics to Optimize Engineered Pentose Fermentation in *Zymomonas mobilis*

M. Mete Altintas[1], Christina Eddy[2], Min Zhang[2], James D. McMillan[2] and Dhinakar S. Kompala[1]

1. Chemical and Biological Engineering Department, University of Colorado, Boulder, CO
2. Biotechnology Division for Fuels and Chemicals, NREL, Golden, CO

Metabolic Engineering V: Genome to Product, September 19-23, Lake Tahoe, CA

Large Scale Modeling to Optimize Engineered

M. Mete Altintas[1], Christina E

1. Chemical and Biol
2. Biotechno

Metabolic Engine

# of The Non-linear Enzy

Pentose Fermentation

ddy[2], Min Zhang[2], James D. McMilla

ogical Engineering Department, University of C
logy Division for Fuels and Chemicals, NREL,

ering V: Genome to Product, September 19-23,

matic Reaction Kinetics in *Zymomonas mobilis*

n[2] and Dhinakar S. Kompala[1]

olorado, Boulder, CO
Golden, CO

Lake Tahoe, CA